BMC Musculoskeletal Disorders

RESEARCH

Open Access

A novel portable and radiation-free method for assessing scoliosis: an accurate and reproducible study

Hui Wang[1], Yunfeng Zhu[1], Qiyuan Bao[2], Yong Lu[1], Fuhua Yan[1], Lianjun Du[1] and Le Qin[1*]

Abstract

Background This study aimed to evaluate the accuracy and reproducibility of a newly developed portable and radiation-free three-dimensional spine sensing system (3D-SSS) for scoliosis assessment.

Methods A total of 145 patients underwent full-spine imaging using the EOS imaging system, and 3D-SSS data were collected between February 2023 and April 2023. A radiologist used sterEOS software to reconstruct the spine in 3D and obtain the Cobb angle. One radiologist and one orthopedist independently measured the patients using 3D-SSS, with the orthopedist performing two measurements per patient. The 3D-SSS post-processing system automatically generated the Cobb angle.

Results The mean Cobb angles obtained from EOS and 3D-SSS were 13.7 ± 9.9° (0.5∽45.7°) and 12.5 ± 8.6° (0.4∽40°), respectively. The intraclass correlation coefficient (ICC) for reliability between EOS and 3D-SSS was 0.921, indicating excellent agreement. Bland–Altman analysis revealed a bias of -1.171° between EOS and 3D-SSS, with only 10 patients outside the limits of agreement (-8.3∽6.0°). The root mean square error between EOS and 3D-SSS was 3.2°. A strong correlation was observed between the Cobb angles measured by EOS and 3D-SSS ($r = 0.931$, $P < 0.001$). The receiver operating characteristics curve showed that the diagnostic performance of 3D-SSS for scoliosis was 0.953 ($P < 0.001$). The sensitivity, specificity, positive predictive value, and negative predictive value of 3D-SSS for diagnosing scoliosis were 87.8%, 92.1%, 93.5%, and 85.3%, respectively. The intraobserver and interobserver ICCs for Cobb angles derived from 3D-SSS were 0.969 and 0.934, respectively, demonstrating excellent reproducibility.

Conclusions The portable and radiation-free 3D-SSS accurately measured scoliosis and provided highly reproducible data. This system offers a novel method for clinicians to screen and monitor scoliosis in young patients.

Keywords Scoliosis, Portable, Radiation-free, Three-dimensional spine sensing system, Cobb angle

*Correspondence:
Le Qin
ql11880@rjh.com.cn
[1]Department of Radiology, Ruijin Hospital, Shanghai Jiao Tong University School of Medicine, No. 197 Ruijin 2nd Rd, Shanghai 200025, China
[2]Department of Orthopedics, Ruijin Hospital, Shanghai Jiao Tong University School of Medicine, No. 197 Ruijin 2nd Rd, Shanghai 200025, China

Background

Scoliosis is a three-dimensional (3D) deformity of the spine involving the coronal, sagittal, and transverse planes [1]. The etiology of scoliosis is multifactorial, involving genetics, spinal biomechanics, neurology, and biochemistry [2]. One prominent neurological theory suggests that poor postural balance control due to impaired vestibular function contributes to its pathogenesis [2, 3]. From a biochemical perspective, low bone mineral density may increase stress and accelerate curve progression in scoliosis [2, 4]. The most common type is adolescent idiopathic scoliosis (AIS), which occurs between the ages of 11 and 18 years, with a global incidence of 0.47–5.2% [2, 5]. Idiopathic adult scoliosis in patients younger than 40 years often progresses from untreated AIS [6]. Clinically, severe AIS can lead to abnormal appearance, asymmetric thoracic cage, impaired cardiopulmonary function, or spinal cord compression [7, 8]. Early diagnosis and severity evaluation of AIS are therefore critical.

Radiological imaging is commonly used to measure the Cobb angle and evaluate the coronal plane in AIS. Historically, full-spine imaging was obtained by combining multiple X-ray radiographs, which resulted in image distortion and significant radiation exposure to patients. With advances in imaging technology, the EOS imaging system has been introduced for evaluating spinal deformities [9, 10]. EOS offers advantages such as a low radiation dose, the ability to capture biplanar images of the entire body in a standing position, and the capability to reconstruct 3D images [11, 12]. However, EOS has several limitations, including complex operation, exposure to ionizing radiation, high initial costs, and immovable equipment, making it unsuitable for large-scale screening and inconvenient for follow-ups [13].

To address these challenges, a novel portable and radiation-free 3D spine sensing system (3D-SSS) was developed, offering an alternative to X-ray imaging for evaluating scoliosis parameters. The 3D-SSS is designed for extensive scoliosis screening and faster clinical examinations. It uses contact space trajectory measurement technology and a micro-electro-mechanical system (MEMS) sensor to measure spatial angles during dynamic movement. Combined with path distance measurement, the system generates spatial vector curve coordinates of the dorsal spinous process [14]. By integrating terrain scanning data from an equipment balance wheel sensor and digitally mapping these coordinates to a standard 3D spine model, a true 3D digital model of the spine can be constructed [15, 16]. Spinal parameters are then calculated in the coronal plane using a mathematical algorithm. Despite its potential, the clinical utility of 3D-SSS remains unclear.

The present study aimed to evaluate the accuracy and reproducibility of Cobb angle measurements obtained using 3D-SSS in patients suspected of scoliosis.

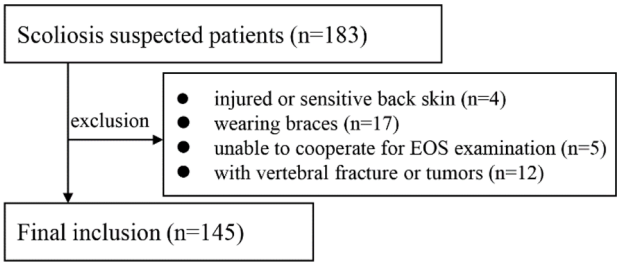

Fig. 1 Flow diagram of patient selection

Methods

Study population

This prospective study was approved by the institutional ethics committee, and all participants provided signed informed consent. Between February 2023 and April 2023, 183 consecutive individuals were enrolled based on the following inclusion criteria: (1) suspected scoliosis; (2) age less than 40 years; (3) underwent full-spine imaging using the EOS imaging system (EOS imaging). Exclusion criteria were as follows: (1) injured or sensitive back skin; (2) use of braces; (3) inability to stand during the EOS examination; (4) presence of vertebral fractures or tumors. Based on these criteria, 38 patients were excluded, leaving a total of 145 patients for analysis (Fig. 1).

EOS imaging and 3D reconstruction

Patients stood at the center of the examination area in the anterior-posterior position with their hands placed in front of their heads. Two images, coronal and sagittal, were simultaneously captured from the head to the femur. Then, a radiologist independently performed 3D reconstruction using sterEOS software in "Fast 3D" mode: (1) The oblique sacral line was identified, and the acetabular position and pelvic inclination were adjusted on the coronal and sagittal images. (2) The curvature of the spine (T1-L5) was determined, and the width of the curvature was adjusted to fit one vertebra. (3) The software automatically generated a model for each vertebral body, which was then manually adjusted to align the terminal lamina, spinous process, and pedicle of the vertebral arch. (4) The apical, upper and lower vertebrae of the Cobb angle were manually identified, and these vertebrae were precisely adjusted. Once the 3D reconstruction was completed, the software automatically calculated the Cobb angle. AIS was defined as a Cobb angle ≥ 10°. Based on treatment recommendations, Cobb angles were classified into three categories: 10∽25° (observation), 25∽45° (brace), and > 45° (surgery).

The measurements were performed by a radiologist with ten years of experience in musculoskeletal radiology using sterEOS software.

Examination with 3D-SSS

The novel 3D-SSS (version: FT07W, Forethought® Spine Data Acquisition and Analysis System, Forethought [Shanghai] Medical Technology Co., Ltd, Shanghai, China) includes a scanning device and a post-processing laptop. The scanning device features a housing, switch, light-emitting diode (LED) indicator, one light-sensitive roller, and four balance rollers on the exterior (Fig. 2). Internally, it contains a MEMS sensor module, an optoelectronic encoder, a mainboard, a battery, and a Bluetooth module. Data analysis and scoliosis measurements are performed using software on the laptop. The MEMS sensor module combines a 3-axis gyroscope, 3-axis accelerometer, and 3-axis geomagnetic sensor, enabling real-time measurements of rotational velocity and acceleration.

When the scanning device moves along the spine, the four balance rollers ensure that the device remains tangent to the spine. The MEMS sensor module detects changes in acceleration and angular velocity in three dimensions (X, Y, and Z). The mainboard's microcontroller unit (MCU) converts the acceleration and angular velocity data into quaternion data, commonly used in 3D motion tracking. The quaternion data is temporarily stored in the MCU's random access memory and is transmitted to the laptop software via the Bluetooth module after the measurement is completed. The laptop software processes the motion data and calculates the Cobb angle.

The operating steps for using the scoliosis detection device are as follows:

(1) The patient stands with straight knees and feet placed upright, facing forward naturally, while wearing thin clothing to ensure accurate measurements.
(2) The operator stands behind the patient and places the device's light-sensitive roller at the level of the C7 vertebra, lightly pressing the balance wheels against the patient's back.
(3) The operator clicks the "START" button on the laptop software and waits for the LED indicator to turn green.
(4) The operator moves the device along the patient's spine from T1 to L5 (Fig. 2). During the movement, the indicator light flashes regularly. The balance wheels remain in contact with the patient's clothing, while the operator uses two fingers to ensure the optoelectric roller remains in contact with the spinal processes.
(5) Upon reaching the L5 level, the device is held stationary for approximately 2 s, allowing the LED

Fig. 2 Illustration and operation of 3D-SSS. (**A**) Housing, switch and LED indicator of the device; (**B**) One light-sensitive roller and four balance rollers of the device; (**C**) Operator moves the device along the patient's spine from T1 to L5

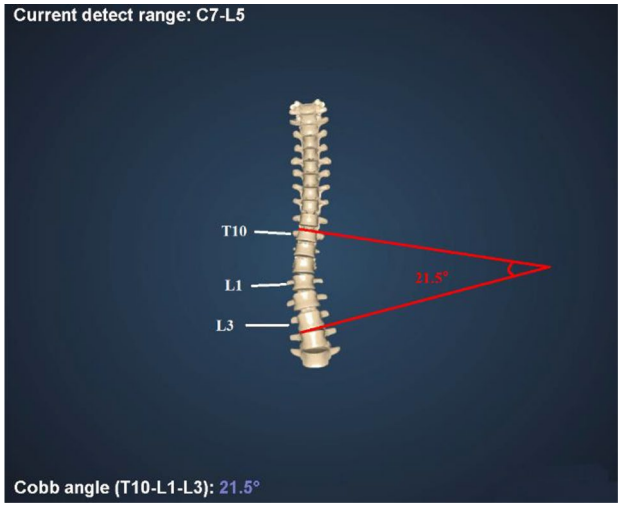

Fig. 3 Reconstruction of spinal 3D model and calculation of Cobb angle by 3D-SSS

Table 1 Demographics of all 145 patients

Age (years old)	19.9 ± 8.7
Sex (Male/female)	51/94
Body mass index (kg/m^2)	19.4 ± 2.3
Initial radiological evaluation for scoliosis (N, %)	82, 56.6%

indicator to stop flashing. The measurement process is then complete.

(6) The device transmits the measurement data to the laptop software, which displays the test results within 3–10 s (Fig. 3).

Subjects were measured independently by two physicians: a radiologist with six years of musculoskeletal radiology experience and an orthopedist with ten years of spine surgery experience. The orthopedist performed two measurements on each subject. Both physicians were blinded to the results obtained from EOS.

Statistical analysis

Quantitative parameters were expressed as mean ± standard deviation. The intraclass correlation coefficient (ICC) was calculated to assess intra- and interobserver variability in the 3D-SSS measurements. ICC values were interpreted as follows: >0.8 (excellent), 0.6–0.8 (good), 0.4–0.6 (moderate), 0.2–0.4 (mild), and < 0.2 (poor reliability). Agreement, reliability, and correlation between measurements from EOS and 3D-SSS were evaluated using Bland–Altman analysis, root mean square error (RMSE), ICC, and Pearson's correlation coefficient, respectively. Statistical analysis was performed using SPSS (version 22.0, IBM, Armonk, NY, USA) and GraphPad Prism (version 8.0.2, GraphPad Software, San Diego, CA, USA). P-value < 0.05 was considered statistically significant.

Results

A total of 145 patients were included in this study. The demographics of all patients are summarized in Table 1. Among these, 82 patients underwent their first X-ray examination for scoliosis detection. The mean age of all patients was 19.9 ± 8.7 years (range: 6∽39 years), with 88 patients aged 18 years or younger (mean: 13.7 ± 2.7 years, range: 6∽18 years). The intra- and interobserver ICCs for the Cobb angle derived from the 3D-SSS were 0.969 (95% CI: 0.957–0.977) and 0.934 (95% CI: 0.909–0.952), respectively, indicating the excellent reproducibility. Bland–Altman analysis (Fig. 4) revealed a bias of 0.1° for intraobserver measurements and – 0.4° for interobserver measurements. Seven and five patients were out of the limits of agreement (LOA) for intraobserver (-4.2∽4.4°) and interobserver (-6.6∽5.8°) measurements, respectively. The RMSE for intra- and interobserver agreement was 2.1° and 3.1°, respectively.

The mean Cobb angle measured by EOS and 3D-SSS was 13.7 ± 9.9° (range: 0.5∽45.7°) and 12.5 ± 8.6° (range: 0.4∽40°), respectively. The absolute difference in Cobb angle between EOS and 3D-SSS was 2.5 ± 2.9°. The reliability of Cobb angle measurements between EOS and 3D-SSS was excellent [ICC = 0.921 (95% CI: 0.893∽0.943)]. Bland–Altman analysis (Fig. 4) indicated a bias of -1.171° between EOS and 3D-SSS, with 10 patients falling outside the LOA (-8.3∽6.0°). The RMSE between EOS and 3D-SSS was 3.2°. Pearson correlation analysis showed a very strong correlation between the Cobb angle measurements obtained using EOS and 3D-SSS ($r = 0.931$, $P < 0.001$). Additionally, the differences in Cobb angle measurements between EOS and 3D-SSS increased with larger Cobb angles, ranging from 1.5° to12.7°as the Cobb angle increased from < 10° to > 45° (Fig. 5).

The diagnostic performance of 3D-SSS for scoliosis (Cobb angle ≥ 10°) is summarized in Table 2. The sensitivity, specificity, positive predictive value, and negative predictive value of 3D-SSS for scoliosis diagnosis were 87.8%, 92.1%, 93.5%, and 85.3%, respectively. Among 63 patients with a Cobb angle < 10°, only 5 were reclassified to a Cobb angle of 10∽25° by 3D-SSS. The receiver operating characteristic (ROC) curve demonstrated the strong predictive ability of 3D-SSS for scoliosis, with an area under the curve (AUC) of 0.953 [95% CI: 0.918∽0.988, $P < 0.001$] (Fig. 6). In 61 patients with a Cobb angle of 10∽25°, 10 were reclassified to a Cobb angle < 10°, and one was reclassified to a Cobb angle of 25∽45° by 3D-SSS. Among 20 patients with a Cobb angle of 25∽45°, 8 were grouped as a Cobb angle of 10∽25° by 3D-SSS. Additionally, 3D-SSS reclassified the only patient with a Cobb angle > 45° to a Cobb angle of 25∽45°. The reclassification results of 3D-SSS are detailed in Table 3.

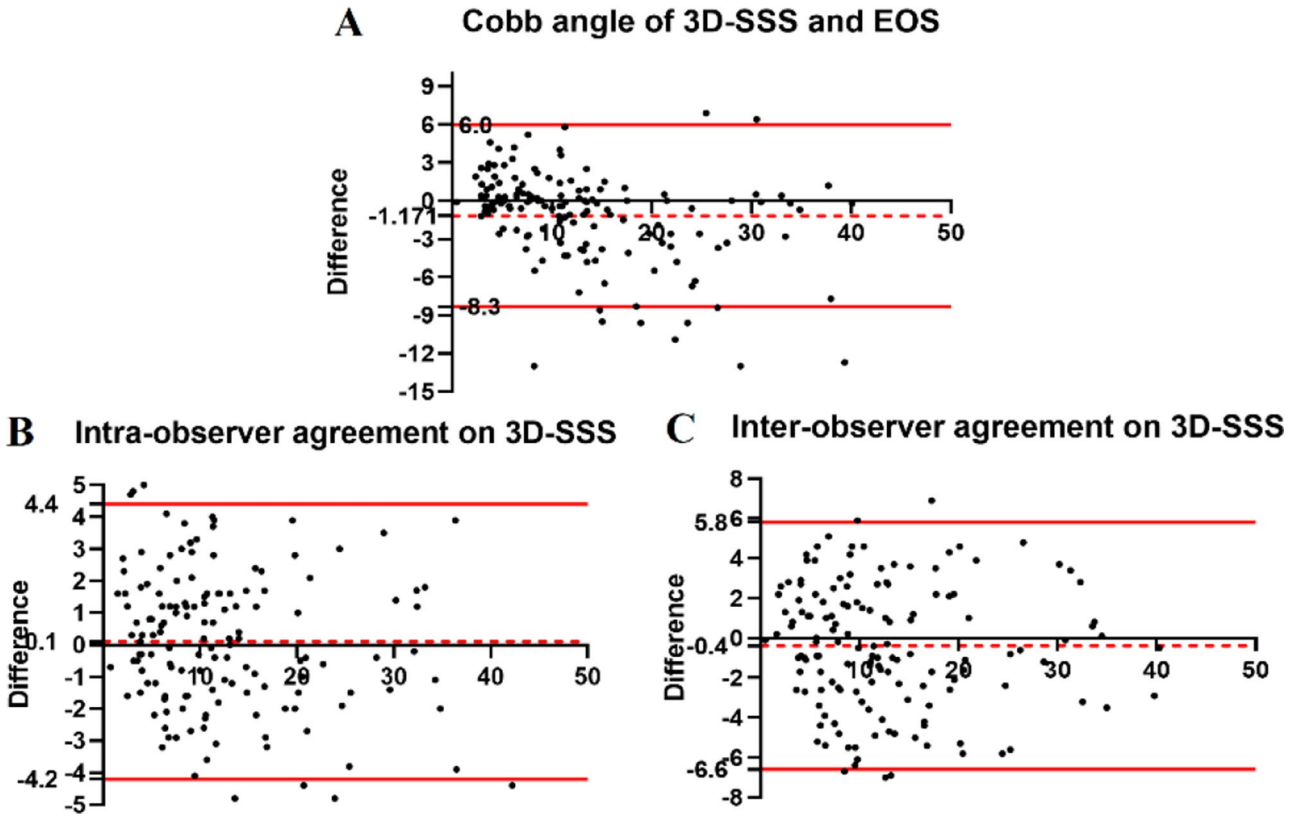

Fig. 4 Bland–Altman analysis of Cobb angle. (**A**) Cobb angle between 3D-SSS and EOS; (**B**) Cobb angle of intraobserver agreement on 3D-SSS; (**C**) Cobb angle of interobserver agreement on 3D-SSS

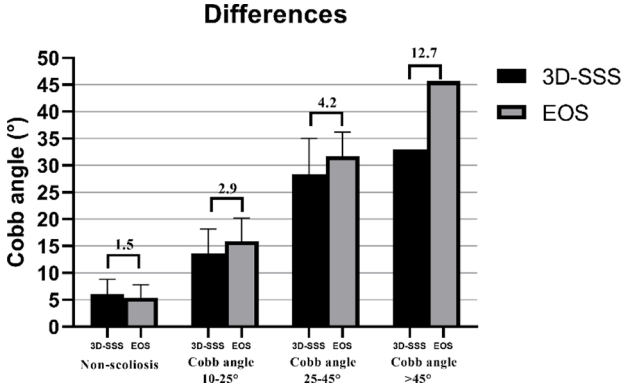

Fig. 5 Differences in Cobb angle between 3D-SSS and EOS

Table 2 Diagnostic ability of scoliosis by 3D-SSS

		EOS		
		Scoliosis	**Non-scoliosis**	**Total**
3D-SSS	Scoliosis	72	5	77
	Non-scoliosis	10	58	68
	Total	82	63	145

3D-SSS: three-dimensional spine sensing system

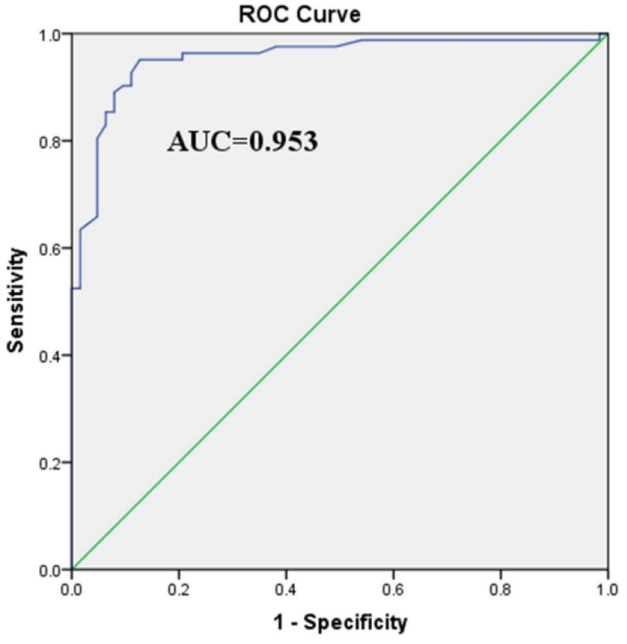

Fig. 6 ROC curves of the diagnostic ability of 3D-SSS for scoliosis

Table 3 Reclassification of the severity of scoliosis by 3D-SSS

EOS			3D-SSS		
Classification	**Patient number**	**Cobb angle**	**Classification**	**Patients number**	**Cobb angle**
Cobb angle < 10°	63	5.4 ± 2.4	Cobb angle < 10°	58	5.6 ± 2.0
			Cobb angle 10–25°	5	12.7 ± 1.7
Cobb angle 10–25°	61	15.9 ± 4.3	Cobb angle < 10°	10	7.8 ± 2.5
			Cobb angle 10–25°	50	14.4 ± 3.6
			Cobb angle 25–45°	1	28.9
Cobb angle 25–45°	20	3.17 ± 4.5	Cobb angle 10–25°	8	21.3 ± 2.5
			Cobb angle 25–45°	12	32.9 ± 3.9
Cobb angle > 45°	1	45.7	Cobb angle 25–45°	1	33.0

3D-SSS: three-dimensional spine sensing system

Discussion

The present study demonstrated that the Cobb angles derived from the automatic reconstruction of 3D-SSS were in good agreement with those obtained by EOS, with excellent intra- and interobserver ICCs for 3D-SSS. These findings indicate that 3D-SSS provides reliable and accurate measurements for scoliosis patients.

Cobb angle is a critical parameter for assessing AIS [17]. Currently, computed radiography and digital radiography are the most common methods for quantitative evaluation of Cobb angle using X-rays. The EOS system has been widely adopted since its introduction, with its feasibility and accuracy in evaluating AIS and adult scoliosis confirmed by previous studies [18–22]. Research has demonstrated a high level of accuracy in Cobb angle measurements obtained from EOS compared to CT in both phantom and patient studies [18, 23, 24]. Consequently, EOS is considered the gold standard for evaluating scoliosis using Cobb angle and axial vertebral rotation (AVR). However, young AIS patients undergoing repeated X-ray exposure face potential harm due to radiation [25].

This study revealed that the Cobb angles measured by the novel portable and radiation-free 3D-SSS are highly consistent with those measured by EOS. Several factors may explain this consistency: (1) The data collection method of 3D-SSS mirrors that of EOS, capturing frontal and lateral spinal parameters simultaneously under weight-bearing conditions, closely reflecting the patient's actual posture in daily life. (2) The system employs a high-precision MEMS sensor that achieves theoretical accuracy values of ≤ 1° in environments free from magnetic interference. (3) The post-processing software automatically matches collected data to each vertebra through sensor fusion algorithms and gain filter control, producing a highly accurate 3D digital spinal model. (4) The post-processing software translates the standard Cobb angle measurement technique (determining the angle between the upper and lower vertebral bodies with maximal inclination in a scoliosis segment) into a mathematical space vector model, automating spinal parameter calculations and reducing manual errors.

Previous studies have investigated various non-X-ray methods for scoliosis detection and Cobb angle assessment. The scoliometer combined with the Adams test is a commonly used manual method in clinical practice, but it lacks objectivity, accuracy, and repeatability [26]. Similarly, portable electronic scoliosis screening device utilize 3D electronic gravity sensing technology to measure the surface trunk rotation and estimate the severity of scoliosis, which may produce false-positive results [27]. In addition, Li et al. proposed a 3D ultrasound method to assess Cobb angle by utilizing ultrasonic technology to image the patient's dorsal spinous processes and reconstruct the spinal morphology. Their study reported a correlation coefficient of > 0.75 between the Cobb angle and the dorsal spinous process, suggesting that ultrasound-based measurements of spinous process sequence can achieve quantitative Cobb angle assessments without X-rays [28]. However, poor probe-skin contact or insufficient coupling gel may impair ultrasound signal transmission, negatively affecting measurement accuracy [29].

Similar to the study by Li et al., this system used the dorsal spinous process as an anatomical reference landmark. However, unlike ultrasound-based methods that locate the spinous process through imaging alone, this system employs a high-precision MEMS combined sensor and contact space trajectory measurement technology. The trajectory space angle measurement module and the path distance measurement module precisely detect the vector position of each spinous process in 3D space. Additionally, terrain scan data from the balance wheel optimize the measurement by accounting for the inclination and torsion of the spinous process caused by the tension of back muscles and fat tissue. Finally, the digital mapping of data, processed through fusion algorithms and gain control, generates a 3D spinal model closely matching the patient's spine, enabling the calculation and analysis of the Cobb angle [30, 31]. This approach, combining 3D vector localization and dorsal spinous process topographic scanning, appears to be more effective than ultrasound alone in locating the coronal spinous process and evaluating the Cobb angle.

The findings of this study have several clinical implications. AIS often presents without distinct symptoms, increasing the risk of missed or delayed diagnosis. Early scoliosis detection through imaging screening allows for timely intervention, such as bracing or surgical procedures [25]. While EOS is accurate and reliable for scoliosis evaluation, its use is limited to specialized examination rooms and requires operation by trained radiographers. EOS also has drawbacks, including high initial costs, relatively long examination times, and radiation exposure, making it unsuitable for large-scale AIS screening [11, 32]. The device used in this study, in contrast, is portable, radiation-free, and cost-effective. The initial setup cost of an EOS system is approximately $509,480, with a per-scan cost of $11.58 [32]. In comparison, the procurement cost of the 3D-SSS is about $41,430, and the per-patient cost is approximately $4.14, both significantly lower than those of EOS. Furthermore, this study found strong consistency and correlation between measurements obtained from 3D-SSS and EOS, along with the high diagnostic accuracy of 3D-SSS, making it suitable for AIS screening in communities, schools, and primary care settings. Early detection of scoliosis through tools like scoliometers enables timely non-operative interventions such as bracing, which can slow progression [33, 34], and surgery at appropriate stages to avoid complications associated with advanced scoliosis [35]. The novel 3D-SSS device also has potential for monitoring disease progression and treatment outcomes, with prognostic implications. Additionally, the device's software provides results within 10 s, expediting clinical diagnosis and management. Therefore, the radiation-free device offers a practical and efficient tool for scoliosis evaluation.

However, the study has some limitations: (1) The sample size was small, particularly for patients with severe Cobb angle deformities. Future studies should include more patients with severe deformities. (2) The influence of the 3D-SSS on clinical treatment strategies was not assessed. For example, patients recommended for surgery based on EOS might be treated with bracing according to 3D-SSS, potentially affecting curve correction. Conversely, patients recommended for observation based on EOS might be overtreated with bracing. Further studies are needed to evaluate the clinical implications. (3) The study lacked follow-up data, preventing comparisons of the same patient over time. (4) Only two physicians (a radiologist and an orthopedist) performed the examinations. Future studies should involve multiple operators to assess the system's consistency. (5) Although promising results were obtained with patients wearing thin clothing, future studies should investigate whether measurements improve with direct skin contact.

Conclusions

In conclusion, 3D-SSS provides accurate and reproducible scoliosis evaluations in adolescents and young adults, with measurements highly consistent with EOS. This system can complement EOS and assist clinicians in diagnosing scoliosis quickly and accurately. However, further validation is needed for patients with severe Cobb angles.

Abbreviations

3D-SSS	Three-dimensional spine sensing system
3D	Three-dimensional
AIS	Adolescent idiopathic scoliosis
MEMS	Micro-electro-mechanical system
LED	Light emitting diode
MCU	Microcontroller unit
ICC	Intraclass correlation coefficient
RMSE	Root mean square error
LOA	Limits of agreement
ROC	Receiver operating characteristic
AUC	Area under the curve
CI	Confidence interval
BMI	Body mass index

Acknowledgements

Not applicable.

Author contributions

All authors read and approved the final manuscript. Hui Wang: drafted the work Fengyun Zhu: the acquisition, analysis, and interpretation of data Qiyuan Bao: the acquisition, analysis, and interpretation of data Yong Lu: the acquisition, analysis, and interpretation of data Fuhua Yan: the concept and the design of the work Lianjun Du: substantively revised the work Le Qin: the concept and the design of the work, substantively revised the work.

Funding

This study was funded under National Key R&D Program of China (2023YFC2410704) and National Natural Science Foundation of China (82171891).

Data availability

The datasets used and analyzed during the current study are available from the corresponding author on reasonable request.

Declarations

Ethics approval and consent to participate

Ethics approval and consent was obtained from Ruijin Hospital Ethics Committee Shanghai JiaoTong University School of Medicine. The reference number is No. (2022)(273). Only if the study is on human subjects: Written informed consent was obtained from all subjects (patients) or their legal guardians in this study.

Consent for publication

Not applicable.

Competing interests

The authors declare no competing interests.

Received: 19 March 2024 / Accepted: 11 February 2025
Published online: 26 February 2025

References

1. Marya S, Tambe AD, Millner PA, Tsirikos AI. Adolescent idiopathic scoliosis: a review of aetiological theories of a multifactorial disease. Bone Joint J. 2022;104:915–21.

2. Peng Y, Wang SR, Qiu GX, Zhang JG, Zhuang QY. Research progress on the etiology and pathogenesis of adolescent idiopathic scoliosis. Chin Med J. 2020;133:483–93.
3. Guo X, Chau WW, Hui-Chan CW, Cheung CS, Tsang WW, Cheng JC. Balance control in adolescents with idiopathic scoliosis and disturbed somatosensory function. Spine. 2006;31(14):e437–40.
4. Song XX, Jin LY, Li XF, Qian L, Shen HX, Liu ZD, et al. Effects of low bone mineral status on biomechanical characteristics in idiopathic scoliotic spinal deformity. World Neurosurg. 2018;110:e321–9.
5. Konieczny MR, Senyurt H, Krauspe R. Epidemiology of adolescent idiopathic scoliosis. J Child Orthop. 2013;7:3–9.
6. Aebi M. The adult scoliosis. Eur Spine J. 2005;14:925–48.
7. Cheng JC, Castelein RM, Chu WC, et al. Adolescent idiopathic scoliosis. Nat Rev Dis Primers. 2015;1:15030.
8. Weinstein SL, Dolan LA, Spratt KF, Peterson KK, Spoonamore MJ, Ponseti IV. Health and function of patients with untreated idiopathic scoliosis. A 50-year natural history study. JAMA. 2003;289:559–67.
9. Dubousset J, Charpak G, Skalli W, Deguise J, Kalifa G. EOS: a new imaging system with low dose radiation in standing position for spine and bone & joint disorders. J Musculoskelet Res. 2010;13:1–12.
10. Harada GK, Siyaji ZK, Younis S, Louie PK, Samartzis D, An HS. Imaging in spine surgery: current concepts and future directions. Spine Surg Relat Res. 2019;4:99–110.
11. Garg B, Mehta N, Bansal T, Malhotra R. EOS imaging: concept and current applications in spinal disorders. J Clin Orthop Trauma. 2020;11:786–93.
12. Luo TD, Stans AA, Schueler BA, Larson AN. Cumulative radiation exposure with EOS imaging compared with standard spine radiographs. Spine Deform. 2015;3:144–50.
13. Melhem E, Assi A, El Rachkidi R, Ghanem I. EOS biplanar X-ray imaging: concept, developments, benefits, and limitations. J Child Orthop. 2016;10:1–14.
14. Algamili AS, Khir MHM, Dennis JO, et al. A review of actuation and sensing mechanisms in MEMS-based sensor devices. Nanoscale Res Lett. 2021;16:16.
15. Sabatini AM. Estimating three-dimensional orientation of human body parts by inertial/magnetic sensing. Sensors. 2011;11:1489–525.
16. Carmi A, Oshman Y. Adaptive particle filtering for spacecraft attitude estimation from vector observations. J Guid Control Dynam. 2009;32:232–41.
17. Rigo M. Patient evaluation in idiopathic scoliosis: radiographic assessment, trunk deformity and back asymmetry. Physiother Theory Pract. 2011;27:7–25.
18. Al-Aubaidi Z, Lebel D, Oudjhane K, Zeller R. Three-dimensional imaging of the spine using the EOS system: is it reliable? A comparative study using computed tomography imaging. J Pediatr Orthop B. 2013;22:409–12.
19. Rehm J, Germann T, Akbar M, et al. 3D-modeling of the spine using EOS imaging system: inter-reader reproducibility and reliability. PLoS ONE. 2017;12:1–13.
20. Okamoto M, Jabour F, Sakai K, Hatsushikano S, Le Huec JC, Hasegawa K. Sagittal balance measures are more reproducible when measured in 3D vs in 2D using full-body EOS images. Eur Radiol. 2018;28:4570–7.
21. Chan AC, Morrison DG, Nguyen DV, Hill DL, Parent E, Lou EH. Intra- and interobserver reliability of the Cobb angle-vertebral rotation angle-spinous process angle for adolescent idiopathic scoliosis. Spine Deform. 2014;2:168–75.
22. Kim SB, Heo YM, Hwang CM, et al. Reliability of the EOS imaging system for assessment of the spinal and pelvic alignment in the sagittal plane. Clin Orthop Surg. 2018;10:500–7.
23. Glaser DA, Doan J, Newton PO. Comparison of 3-dimensional spinal reconstruction accuracy: biplanar radiographs with EOS versus computed tomography. Spine (Phila Pa 1976). 2012;37:1391–7.
24. Carreau JH, Bastrom T, Petcharaporn M, et al. Computer-generated, three-dimensional spine model from biplanar radiographs: a validity study in idiopathic scoliosis curves greater than 50 degrees. Spine Deform. 2014;2:81–8.
25. Rigo MD, Villagrasa M, Gallo D. A specific scoliosis classification correlating with brace treatment: description and reliability. Scoliosis. 2010;5:1–11.
26. Fong DY, Lee CF, Cheung KM, et al. A meta-analysis of the clinical effectiveness of school scoliosis screening. Spine (Phila Pa 1976). 2010;35:1061–71.
27. Li C, Zhang B, Liu L, et al. Design, reliability, and validity of a portable electronic device based on ergonomics for early screening of adolescent scoliosis. J Orthop Translat. 2021;28:83–9.
28. Li M, Cheng J, Ying M, Ng B, Lam TP, Wong MS. A preliminary study of estimation of Cobb's angle from the spinous process angle using a clinical ultrasound method. Spine Deform. 2015;3:476–82.
29. Lai KK, Lee TT, Lee MK, Hui JC, Zheng YP. Validation of scolioscan air-portable radiation-free three-dimensional ultrasound imaging assessment system for scoliosis. Sensors(Basel). 2021;21:2858–75.
30. Giansanti D, Macellari V, Maccioni G, Cappozzo A. Is it feasible to reconstruct body segment 3-D position and orientation using accelerometric data? IEEE Trans Biomed Eng. 2003;50:476–83.
31. Cortell-Tormo JM, Garcia-Jaen M, Ruiz-Fernandez D, Fuster-Lloret V. Lumbatex: a wearable monitoring system based on inertial sensors to measure and control the lumbar spine motion. IEEE Trans Neural Syst Rehabil Eng. 2019;27:1644–53.
32. Faria R, McKenna C, Wade R, Yang H, Woolacott N, Sculpher M. The EOS 2D/3D X-ray imaging system: a cost-effectiveness analysis quantifying the health benefits from reduced radiation exposure. Eur J Radiol. 2013;82:342–9.
33. Diebo BG, Segreto FA, Solow M, et al. Adolescent idiopathic scoliosis care in an underserved inner-city population: screening, bracing, and patient- and parent-reported outcomes. Spine Deform. 2019;7:559–64.
34. Grossman DC, Curry SJ, Owens DK, et al. Screening for adolescent idiopathic scoliosis: US preventive services task force recommendation statement. JAMA. 2018;319:165–72.
35. Adobor RD, Rimeslatten S, Steen H, Brox JI. School screening and point prevalence of adolescent idiopathic scoliosis in 4000 Norwegian children aged 12 years. Scoliosis. 2011;6:1–7.

Publisher's note